

Customized edge cutting of display glass with laser-only machining

Myriam Kaiser,^a Jonas Kleiner,^a  Jannis Wolff,^a and Daniel Flamm^a 

^aTRUMPF Laser- und Systemtechnik GmbH, Johann-Maus-Str. 2, 71254 Ditzingen, Germany

ABSTRACT

Cleaving of glass substrates with shaped edges using a laser-only concept is presented. In a first laser process shaped ultrashort laser pulses modify in a single pass the entire material thickness with arbitrary edge shape geometries. Afterwards in a second pass CO₂ laser radiation is absorbed in the modified area and resulting stresses lead to the separation of the glass. We investigate the quality of the achieved edges and corresponding mechanical properties. The cutting strategy, so far conducted on straight contours, is successfully transferred to curved contours maintaining edge qualities.

Keywords: Beam shaping, ultrafast optics, laser materials processing, glass processing, structured light

1. INTRODUCTION

Conventional glass cutting processes are usually limited to orthogonal glass edges.^{1–3} Stresses accumulate in the right-angled corners of such edges and the glass can easily break on impact.^{4,5} By reducing the tangential angle at the glass surface through grinding and polishing the resistance to impact can be increased.^{5–7} Using ultra-short pulse laser-based glass cutting techniques with state-of-the-art Bessel like beams, intrinsically vertical glass edges result.^{8–10} But strong advantages such as quality, tool wear, throughput, and the ability for contour cuts speak in favor of the laser-based approach. These advantages and the possibility to generate modifications in a single pass over the entire material thickness along any edge shape geometry are united using holographic 3D beam splitters.^{5,11} This optical concept enables arranging a large number of focus copies arbitrarily within the glass substrate.

After the laser modification step a second step follows, that separates along the multispot modifications weakened areas of the material. In contrast to selective etching separation,^{12–15} thermal separation with CO₂ laser radiation^{7,16–18} has the advantage of using another non-contact tool and is, additionally, characterized by low costs. Considering fabrication of consumer-electronics-relevant cover glasses we assume that CO₂ laser-based separation is four times cheaper than concepts based on selective laser etching. Further advantages relate to occupational safety and environmental protection. Radiation from CO₂ lasers operating at 10.6 μm with nanosecond pulses or longer is applied to the glass surface and absorbed close to the area where the ultrafast laser was inducing type-III-regime modifications.^{19,20} Due to the temperature changes in the material, stresses arise that finally lead to the separation of the glass.^{3,21} We would like to point out that the success of this separation strategy strongly depends on the type of glass and, in particular, on the linear thermal expansion coefficients α_L . Fused silica, for example, is characterized by $\alpha_L^{\text{FS}} = 0.6 \cdot 10^{-6} \text{ K}^{-1}$.²² Here, CO₂ laser-based separation strategies are practically impossible or require multiple passes with high thermal loads, where there is a high risk of altering the material. On the other hand, soda-lime glass—as the most prevalent glass type—exhibits an $\alpha_L^{\text{SL}} \approx 14 \cdot \alpha_L^{\text{FS}}$ is, thus, very sensitive to temperature changes²³ and enables separation via thermal stress even for large substrate thicknesses. Display cover glasses typically exhibit thicknesses of $\sim 0.5 \text{ mm}$ and are often fabricated from scratch-resistant Corning[®] Gorilla[®] substrates.²⁴ Due to a thermal expansion behavior $\alpha_L^{\text{GOR}} \approx \alpha_L^{\text{SL}}$ ²⁴ we expect a similarly high suitability for thermal separation processes.

In what follows, we will describe the laser-optical approach for inducing modifications along arbitrary curved trajectories within the bulk of the transparent substrate. Furthermore we will present separation results from applying CO₂ radiation to the volume-modified samples and discuss corresponding laser parameters. We demonstrate first promising four-point-bending-test results of C-shaped glass edges and provide an outlook for separating complex display contours.

Further author information:

E-Mail: myriam.kaiser@trumpf.com.

© 2024 Society of Photo-Optical Instrumentation Engineers (SPIE). One print or electronic copy may be made for personal use only. Systematic reproduction and distribution, duplication of any material in this publication for a fee or for commercial purposes, and modification of the contents of the publication are prohibited.

Frontiers in Ultrafast Optics: Biomedical, Scientific, and Industrial Applications XXIV © 2024 SPIE.

<https://doi.org/10.1117/12.3000909>.

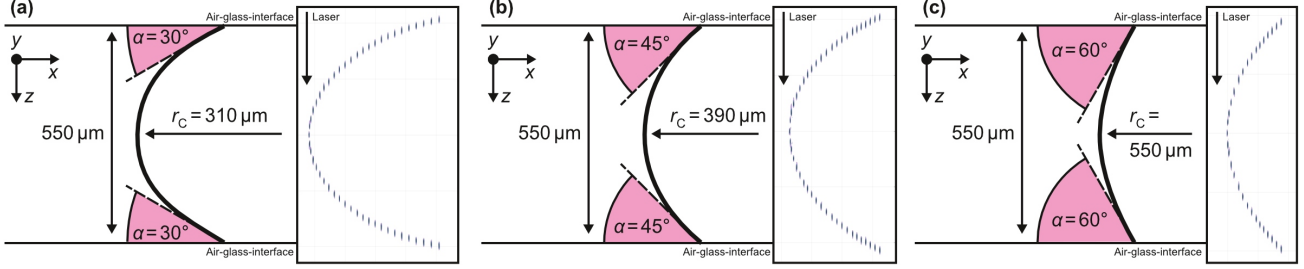


Figure 1. Overview of used focus distributions. The schematic denotes the 550 μm -thick Corning[®] Gorilla[®] sample with both interfaces and the definition of the focus shape’s tangential angle to the surface α . In this work three different C-shapes are to be processed with $\alpha = 30^\circ$ (a), $\alpha = 45^\circ$ (b) and $\alpha = 60^\circ$ (c), and stated radii of corresponding circular arcs r_C . On the right-hand-side of each subfigure the simulated intensity distribution $I(x, z)$ in an isosurface representation is depicted. While laser propagation is parallel to the z -axis, processing is done in y -direction.

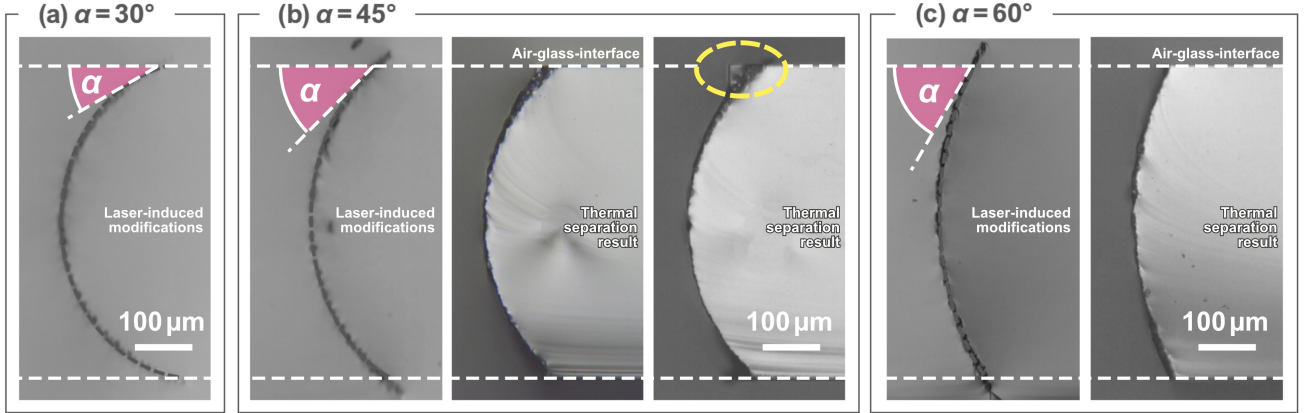


Figure 2. Light micrographs of tailored-edge glass processing and CO₂ laser-based separation. For the 30°-C-shape (a) laser induced modifications follow the circular arc. A thermal separation was not possible. The 45°-C-shape (b) enabled thermal separation with small target geometry deviations close to both interfaces, highlighted in yellow. In the 60° case modifications and resulting edge shape clearly follow the target shape, cf. Fig. 1.

2. SEPARATION OF MULTI-SPOT-MODIFIED GLASSES WITH CO₂ LASERS

Recently, the concept of holographic-3D beam splitters, also called “Photonic shaping tools” was introduced.^{5,11} Here, focus copies can be used to deposit energy at arbitrary positions in a working volume of a lens.^{25–28} For the task at hand, three different focus distributions have been designed. All take the shape of a “C” and are defined for a glass thickness of 550 μm . The spatial trajectory at which foci are split equals a circular arc with a given radius r_C . This radius was chosen so that the arc’s tangent at the intersection with the top and bottom surface equals $\alpha = 30^\circ, 45^\circ$ and 60° . Figure 1 provides an overview of the three cases and shows the simulated intensity distribution $I(x, z)$ of the designed focus, see right-hand-side of (a)–(c). Clearly visible are the spatially separated Gaussian-like spots with similar peak intensities. Please note, that not all spots are visible as an intensity cross section is plotted. During the processing a relative movement of workpiece and processing head is carried out in y -direction. Ultrashort laser pulses propagate parallel to the z -axis and are generating all spots simultaneously in a single pass—a flipping of the workpiece is not required.⁵ Processing was conducted with 3 ps pulses from a [TruMicro Series 2000 laser](#) operating in burst-mode with a total pulse energy of $< 300 \mu\text{J}$. For the thermal separation step a pulsed CO₂ laser system (Synrad p400, Novanta PHOTONICS) with a feed rate of $\sim 3 \text{ m/min}$ at $< 40 \text{ W}$ average power was employed.

Figure 2 depicts processing results with the three focus shapes. For the 30°-case only a light microscope signal of the ultrafast laser-induced modifications is provided. Although the void chain follows the desired trajectory, in this particular case, a thermal separation was not possible, see (a). In Fig. 2 (b), we increased α to 45°. Again, as by design, our focus shape allows to deposit energy along the 45°-arc proven by the type-III-regime modifications visible with light microscopy. Now, thermal substrate separation is enabled as can be seen from

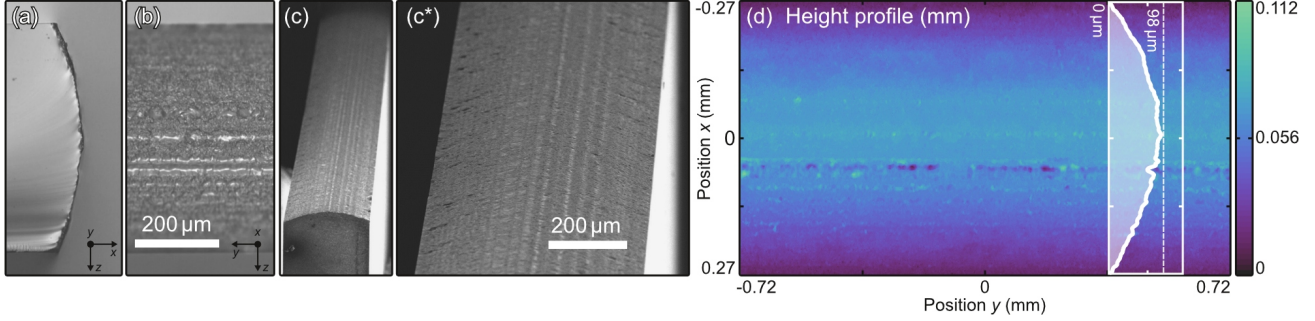


Figure 3. Investigating shape and surface quality of a C-shaped Corning Gorilla glass sample with $\alpha = 60^\circ$ separated by means of CO2 laser radiation, cf. Fig. 2(c). Light microscope signals from different perspectives, note the coordinate system (a), (b). Scanning electron microscopy of the tailored edge (c) with details of the surface grooves (c*). Height profile of the glass edge in 2D and 1D reconstructed from a laser scanning microscope.

the microscoped edges. They largely follow our design, especially at the vertex of the C-shape in the center of the substrate. However, considering the edge shape close to the air-glass-interface larger deviations become visible. In a z -distance of a few tens-of-micrometers away from both interfaces separation is no longer guided along the modifications, but takes the direct path to both surfaces. This often results in an isolated stair step, highlighted in yellow, see (b). Although, due to the local 90° angle, edge protection is no longer guaranteed,⁵ we still see high potential here. This is especially due to the fact that post-treatment by mechanical grinding and polishing¹ is not excluded. The preforming that we can achieve with our double-laser process should significantly reduce the effort required for accuracy and process times of the grinding tools. Optimal chamfering of transparent workpieces could therefore also be achieved by combining laser processing and mechanical post-treatment. However, as described in the introduction, we are looking for a pure laser process and, therefore, use the C-shape with 60° tangential angle, see Fig. 2(c). Here, a broad process window can be found, where the substrate separates without showing steps. The edge closely follows our target trajectory and separation is completely performed along the induced modifications.

A more detailed examination of the sample obtained is carried out by scanning electron microscopy (SEM) and laser scanning microscopy, respectively, see Fig. 3. Here, for the sake of completeness we again plot the light microscope signal of the edge from two perpendicular perspectives, (a) and (b). One outcome of our processing strategy with discrete focal spots is the existence of smallest grooves parallel to the feed direction (y -axis). However, the 3D impression from the SEM image shows that the grooves are very shallow and can be assigned to the transverse dimensions of the spots, see (c) and corresponding details in (c*). The reconstructed height profile from the LSM is depicted in (d). Here, surface roughness S_a is determined to $\approx 2 \mu\text{m}$ and the edge's tangential angle at the air-glass-interfaces amounts to $\alpha = (60 \pm 5)^\circ$, cf. Fig. 1. Fitting the white profile denoted in Fig. 3(d) to a circular arc results in radius of $r_C^{\text{fit}} \approx 510 \mu\text{m}$ (least square method). The fact that this value is slightly smaller than our target value of $550 \mu\text{m}$ is due to the propagation direction of the split spots. Regardless of the position along our C-trajectory, whether at the vertex or at the glass interface, the propagation direction of the focal points is always parallel to the z -axis, cf. Fig. 1. As the Rayleigh lengths are larger than the focus diameter, the resulting modifications at the glass edge protrude more into the sample's good part than those at the vertex, cf. Fig. 2, resulting in a reduced r_C , see also Ref. 5. However, this small mismatch could be compensated in the trajectory design, for example, by slightly increasing r_C .

3. MECHANICAL PROPERTIES OF THERMALLY SEPARATED SAMPLES

With the previous section, the proof-of-concept was provided, that tailored glass edges can be fabricated with laser-only machining. However, the question remains as to what extent our double laser processing strategy is influencing the material's mechanical properties. Here, we follow the argumentation of Marjanovic *et al.*⁴ that glass substrates with chamfered edges will exhibit improved impact resistances. However, this is technologically complex to prove and should also be carried out on the hardened substrate. We therefore choose the detour of testing the substrate's bending strength via four-point-bending tests.¹ If bending strength is not reduced compared to samples with conventionally produced edges, improved impact properties can be expected.^{4,5}

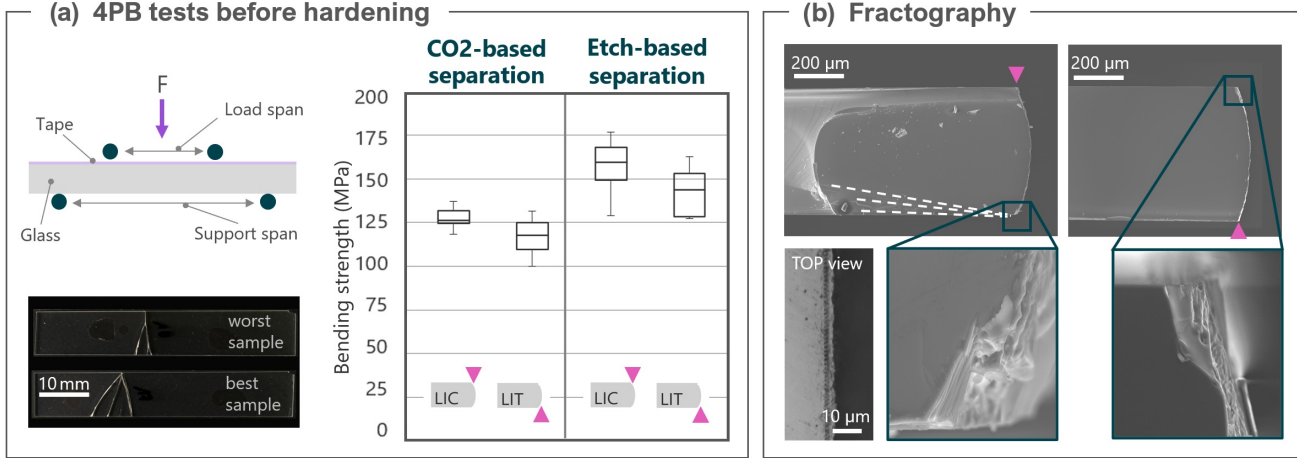


Figure 4. Testing the mechanical properties laser-only machined C-shaped glass substrates. Four-point-bending test arrangement with definition of loading pin position to the substrate’s edge (a). Measured bending strength of two sets of samples separated via CO₂ laser radiation and selective laser etching, respectively, see box plots. Analysis of the breaking behavior with fractography^{29,30} analysis revealing the origin of crack propagation from the intersection of the C-shaped trajectory with the surface under tension (b).

Four-point bending tests are conducted on two set of samples. The first set comprises 550 μm-thick Corning® Gorilla® glass substrates with 60°-C-shaped edges, cf. Fig. 2(c), fabricated from laser-only machining. As reference, the same material and geometry is used, but separated from selective laser etching (SLE).^{31,32} In order to determine the influence of the laser entry and exit side during load application, laser incident sides for both set of samples were tested under compression (LIC) and tension (LIT), Fig. 4(a). Here, too, a schematic of the bending test arrangement is depicted where the orientation of the loading pins to the substrate’s processed edge is defined.

Results of the bending tests are box-plotted in Fig. 4(a). With median bending strengths of ≈ 125 MPa, the CO₂ separated samples show similar mechanical properties as of substrates fabricated via SLE serving as best-in-class processing strategy. It is assumed that the 20% edge strength reduction for the CO₂-processed samples is caused by discontinuities in the edge surface being polished during etching step, resulting in slightly increased bending strengths for the SLE samples. To foster understanding a fractography analysis²⁹ of the CO₂-separated samples was carried out, cf. Fig. 4(b). Considering the fracture mirrors of the broken edges for both cases, LIC and LIT samples, the origin of the crack propagation is at the intersection of the “C” with the surface under tension. In the top view of these surfaces modifications of the last spots in the C-shape focus distribution are still visible. This incomplete separation with partial chipping favors crack propagation and causes reduced breaking strengths. We assume that further optimizations of the focus distribution can improve the mechanical properties of the laser-only processed glass substrates in order to reach the level of SLE processed samples, cf. Fig. 4.

4. CUTTING COMPLEX CONTOURS

Laser-based glass cutting is superior to conventional scribe-and-break techniques when complex contours need to be cut. So far, for our fundamental investigations we have fabricated and investigated samples with straight contours, cf. Fig. 5(a). We therefore expand our processing strategy and cut samples along curved outer contours by translating the workpiece relative to the optical head in the two transverse (x, y) directions, cf. Fig. 1. Again, the processing strategy consists of in-volume modifications from ultrafast lasers and subsequent separation from CO₂ laser induced thermal stress, cf. Sec. 2. Both processing steps require only one laser pass each. A schematic of the simple outer contour at which we want to cut the 550 μm-thick Corning Gorilla glass substrate is shown in Fig. 5(b). Here, a radius-of-curvature of ~ 10 mm was chosen. To enable separation, we add assist modification lines to the target contour and achieve the depicted sample, see photograph in (b). The SEM investigated edge proves a successful C-shape with a quality similar to those from samples cut along straight contours (a).

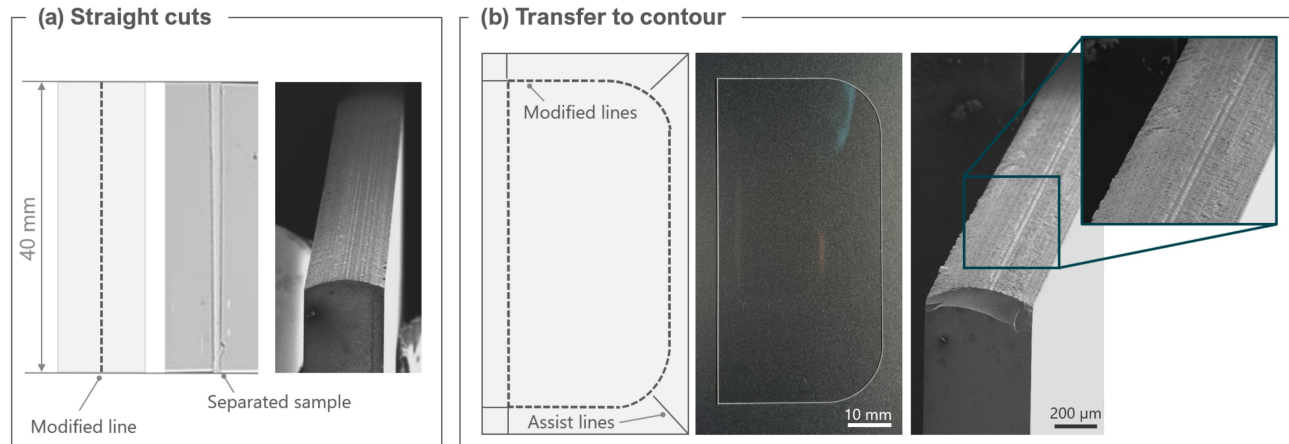


Figure 5. Transferring the laser-only cutting and edge-chamfering of glass substrates from straight cuts (a) to more complex contours (b). In both cases signals from light microscopy and scanning electron microscopy confirm a successful separation process of 550 μm -thick Corning[®] Gorilla[®] glass samples.

Noticeable, the edge shape including smallest groove features caused by our discrete focus distribution are visible, too. We therefore conclude that, in general, the two-step, laser-only process can also be transferred to more complex contours.

With the machining results presented here, we do not claim to have found the optimum. However, these show promising initial trials, with the associated laser parameters providing the basis for further investigations. However, we see a clear correlation between the pulse energy used, the spatial pulse distance and the required average power of the CO₂ laser radiation. A certain fill factor in our focus distribution (ratio of spot size to spot distance) will, for specific laser parameters, cause the resulting modifications to provide crack guidance along the target edge geometry.

5. CONCLUSION

We have demonstrated glass cutting and edge shaping with laser-only machining. The two-step process requires single-pass in-volume modifications from ultrashort laser pulses spatially shaped with a holographic 3D beam splitter. With a second step, the substrate's separation is achieved by inducing thermal stress from CO₂ laser radiation. Glass edges processed can exhibit different shapes and follow, for example, C-shapes with controllable radii-of-curvatures. Most robust processing was achieved with focus distributions that result in tangential angles of $\sim 60^\circ$ at the entrance/exit surface. Here, surface roughnesses of $\sim 2 \mu\text{m}$ have been determined. In addition to the investigation of the edge shape and surface qualities, bending strengths were measured using four-point-bending tests. Here, strength values are similar to those known from substrates processed with selective laser etching. Finally, the concept, so far conducted on straight contours, was successfully transferred to more complex contours with consistent edge qualities.

REFERENCES

1. P. Bukieda, K. Lohr, J. Meiberg, and B. Weller, "Study on the optical quality and strength of glass edges after the grinding and polishing process," *Glass Structures & Engineering* **5**, pp. 411–428, 2020.
2. M. Zhou, B. Ngoi, M. Yusoff, and X. Wang, "Tool wear and surface finish in diamond cutting of optical glass," *Journal of Materials Processing Technology* **174**(1-3), pp. 29–33, 2006.
3. S. Nisar, L. Li, and M. Sheikh, "Laser glass cutting techniques—a review," *Journal of Laser Applications* **25**(4), p. 042010, 2013.
4. S. Marjanovic, D. Andrew, P. Garrett, A. Piech, J. M. Quintal, H. Schillinger, S. Tsuda, R. S. Wagner, and A. N. Yeary, "Edge chamfering methods," Oct. 15 Oct. 15 2019. US Patent 10,442,719.

5. D. Flamm, M. Kaiser, M. Feil, M. Kahmann, M. Lang, J. Kleiner, and T. Hesse, "Protecting the edge: Ultrafast laser modified C-shaped glass edges," *Journal of Laser Applications* **34**(1), p. 012014, 2022.
6. D. Sohr, J. U. Thomas, and S. Skupin, "Shaping convex edges in borosilicate glass by single pass perforation with an Airy beam," *Optics Letters* **46**(10), pp. 2529–2532, 2021.
7. C. Ungaro and A. Liu, "Single-pass cutting of glass with a curved edge using ultrafast curving bessel beams and oblong airy beams," *Optics & Laser Technology* **144**, p. 107398, 2021.
8. W.-J. Tsai, C.-J. Gu, C.-W. Cheng, and J.-B. Horng, "Internal modification for cutting transparent glass using femtosecond bessel beams," *Optical Engineering* **53**(5), pp. 051503–051503, 2014.
9. M. Kumkar, M. Kaiser, J. Kleiner, D. Grossmann, D. Flamm, K. Bergner, and S. Nolte, "Ultrafast laser processing of transparent materials supported by in-situ diagnostics," in *Laser Applications in Microelectronic and Optoelectronic Manufacturing (LAMOM) XXI*, **9735**, p. 97350P, International Society for Optics and Photonics, 2016.
10. M. Jenne, D. Flamm, K. Chen, M. Schäfer, M. Kumkar, and S. Nolte, "Facilitated glass separation by asymmetric Bessel-like beams," *Optics Express* **28**(5), pp. 6552–6564, 2020.
11. D. Flamm, J. Hellstern, M. Kaiser, M. Kahmann, J. Kleiner, and C. Tillkorn, "Light along curves: Photonic shaping tools," *Adv. Opt. Techn.* **12**, 2023.
12. M. Kaiser, M. Kumkar, R. Leute, J. Schmauch, R. Priester, J. Kleiner, M. Jenne, D. Flamm, and F. Zimmermann, "Selective etching of ultrafast laser modified sapphire," in *Laser Applications in Microelectronic and Optoelectronic Manufacturing (LAMOM) XXIV*, **10905**, p. 109050F, International Society for Optics and Photonics, 2019.
13. J. Gottmann, M. Hermans, N. Repiev, and J. Ortmann, "Selective laser-induced etching of 3D precision quartz glass components for microfluidic applications—up-scaling of complexity and speed," *Micromachines* **8**(4), p. 110, 2017.
14. Y. Bellouard, A. Said, M. Dugan, and P. Bado, "Fabrication of high-aspect ratio, micro-fluidic channels and tunnels using femtosecond laser pulses and chemical etching," *Optics express* **12**(10), pp. 2120–2129, 2004.
15. V. Tielen and Y. Bellouard, "Three-dimensional glass monolithic micro-flexure fabricated by femtosecond laser exposure and chemical etching," *Micromachines* **5**(3), pp. 697–710, 2014.
16. M. Mielke, R. A. Srinivas, T. Booth, and T. Wilbanks, "Systems and processes that singulate materials," Mar. 26 2019. US Patent 10,239,160.
17. M. Kumkar, J. Kleiner, D. Großmann, D. Flamm, and M. Kaiser, "System for asymmetric optical beam shaping," Jan. 5 2021. US Patent 10,882,143.
18. M. I. Heiss, U. Stute, and R. J. Terbrueggen, "Apparatuses and methods for synchronous multi-laser processing of transparent workpieces," Feb. 2 2021. US Patent 10,906,832.
19. K. Itoh, W. Watanabe, S. Nolte, and C. B. Schaffer, "Ultrafast processes for bulk modification of transparent materials," *MRS bulletin* **31**(8), pp. 620–625, 2006.
20. D. Flamm, D. Grossmann, M. Kaiser, J. Kleiner, M. Kumkar, K. Bergner, and S. Nolte, "Tuning the energy deposition of ultrashort pulses inside transparent materials for laser cutting applications," *Proc. LiM* **253**, 2015.
21. M. Kumkar, D. Großmann, and D. Flamm, "Diffractive optical beam shaping element," Apr. 14 2020. US Patent 10,620,444.
22. B. Deng, Y. Shi, and F. Yuan, "Investigation on the structural origin of low thermal expansion coefficient of fused silica," *Materialia* **12**, p. 100752, 2020.
23. J. Martin, *Materials for engineering*, Woodhead Publishing, 2006.
24. Corning: Corning® Gorilla® Glass 3. https://www.corning.com/microsites/csm/gorillaglass/PI_Sheets/2020/Gorilla_Glass_3_ProdSheet.pdf. Accessed: 2023-12-29.
25. P. J. Valle, J. E. Oti, V. F. Canales, and M. P. Cagigal, "Multiple coaxial foci generation by phase-only pupil filters," *Optics communications* **272**(2), pp. 325–329, 2007.
26. P. J. Valle and M. P. Cagigal, "Analytic design of multiple-axis, multifocal diffractive lenses," *Optics Letters* **37**(6), pp. 1121–1123, 2012.

27. L. Zhu, M. Sun, M. Zhu, J. Chen, X. Gao, W. Ma, and D. Zhang, “Three-dimensional shape-controllable focal spot array created by focusing vortex beams modulated by multi-value pure-phase grating,” *Optics Express* **22**(18), pp. 21354–21367, 2014.
28. D. Flamm, D. G. Grossmann, M. Sailer, M. Kaiser, F. Zimmermann, K. Chen, M. Jenne, J. Kleiner, J. Hellstern, C. Tillkorn, *et al.*, “Structured light for ultrafast laser micro-and nanoprocessing,” *Optical Engineering* **60**(2), p. 025105, 2021.
29. G. D. Quinn and G. D. Quinn, *Fractography of ceramics and glasses*, vol. 960, National Institute of Standards and Technology Washington, DC, 2007.
30. R. C. Bradt, “The fractography and crack patterns of broken glass,” *Journal of failure analysis and prevention* **11**, pp. 79–96, 2011.
31. M. Hermans, J. Gottmann, and F. Riedel, “Selective, laser-induced etching of fused silica at high scan-speeds using KOH.,” *Journal of Laser Micro/Nanoengineering* **9**(2), 2014.
32. M. Kaiser, H. Dounassre, M. Kahmann, J. Hellstern, J. Kleiner, C. Tillkorn, and D. Flamm, “Chamfered-edge laser cleaving of transparent materials,” in *Frontiers in Ultrafast Optics: Biomedical, Scientific, and Industrial Applications XXII*, **11991**, pp. 32–41, SPIE, 2022.